

(London) 218, 937 (1968)] found dry-season DOC values of 2 to 3.5 g m<sup>-3</sup> downriver.

7. We assume that biogenic oxidation of organic carbon is mainly associated with POC; thus, relative utilization rates are calculated as POC specific respiration, or grams per cubic meter per day divided by grams per cubic meter (with data from Table 1).
8. C. H. Williams and W. J. Junk, *Biogeographica* 7, 115 (1976).
9. T. R. Fisher, *J. Comp. Biochem. Physiol.*, in press.
10. R. C. Wissmar, J. E. Richey, R. F. Stallard, J. M. Edmond, in preparation.
11. R. J. Gibbs, *Geochim. Cosmochim. Acta* 36, 1061 (1972).
12. K. C. Beck, J. H. Reuter, E. M. Perdue, *ibid.* 38, 341 (1974).
13. W. F. Curtis, R. H. Meade, C. F. Nordin, W. B. Price, E. R. Sholkovitz, *Nature (London)* 280, 381 (1979).
14. We estimate the POC load in the 20 largest rivers from the data on total suspended solids of H. D. Holland [*The Chemistry of the Atmosphere and Oceans* (Wiley-Interscience, New York, 1978), p. 86] by assuming that the POC is 5 and 2 percent of the total suspended solids in tropical and nontropical rivers, respectively, and that DOC is an average of 4 g m<sup>-3</sup>; these values yield an estimate of 2 × 10<sup>14</sup> g year<sup>-1</sup> as the input to the oceans. As for the Amazon, corrections for processing and depth-weighting must be applied and organic carbon fractions larger than 1 mm must be included. As the top 20 rivers constitute about 35 percent of the freshwater discharge to the oceans, this estimate would be increased to get the total riverine contribution. The total effective carbon efflux thus is about 10<sup>15</sup> g year<sup>-1</sup>.
15. G. M. Woodwell, R. H. Whittaker, W. A. Reiners, G. E. Likens, C. C. Delwiche, D. B. Botkin, *Science* 199, 141 (1978); W. S. Broecker, T. Taskahashi, H. J. Simpson, T.-H. Peng, *ibid.* 206, 409 (1979).
16. J. E. Hobbie and G. E. Likens, *Limnol. Oceanogr.* 18, 734 (1973); D. L. Lush and H. B. N. Hynes, *Hydrobiologia* 60, 177 (1978); C. Dahm, personal communication.
17. We thank A. H. Devol for assistance with the respiration data, F. Curren and B. Grant for logistics support, and the crew and scientists of the R.V. *Alpha Helix* and the Instituto Nacional Pesquisas Amazonas for their courtesy and cooperation from the National Science Foundation. Supported by grants DEB-76-82631 and BMS-75-07333. Contribution No. 512 from the College of Fisheries, University of Washington, and Contribution No. 9 from the River Continuum project.

20 August 1979; revised 6 December 1979

## Alaskan Seismic Gap Only Partially Filled by 28 February 1979 Earthquake

**Abstract.** *The Saint Elias, Alaska, earthquake (magnitude 7.7) of 28 February 1979 is the first major earthquake since 1900 to occur along the complex Pacific-North American plate boundary between Yakutat Bay and Prince William Sound. This event involved complex rupture on a shallow, low-angle, north-dipping fault beneath the Chugach and Saint Elias Mountains. The plate boundary between Yakutat Bay and Prince William Sound had been identified as a seismic gap, an area devoid of major earthquakes during the last few decades, and was thought to be a likely site for a future major earthquake. Since the Saint Elias earthquake fills only the eastern quarter of the gap, the remainder of the gap to the west is a prime area for the study of precursory and coseismic phenomena associated with large earthquakes.*

On 28 February 1979 an earthquake with surface wave magnitude ( $M_s$ ) 7.7 (1) occurred beneath the Chugach and Saint Elias Mountains about 130 km northwest of Yakutat Bay, Alaska. Earlier, the region between the 1958 Fairweather earthquake ( $M_s$  7.9), which broke the Fairweather fault as far north as Yakutat Bay, and the 1964 Prince William Sound earthquake ( $M_s$  8.4), which ruptured the Aleutian megathrust from about Kodiak Island to Kayak Island, had not been the site of a major earthquake since 1899 and 1900, when four events of  $M_s$  8.5, 7.8, 8.4, and 8.1 occurred within 13 months (2). Although instrumental control for the epicenters of 1899 and 1900 is almost nonexistent, felt reports and observed uplifts place at least three of them between Yakutat Bay and Kayak Island (2, 3). Absence of recent major earthquakes identifies this zone as a seismic gap (4, 5), a region of greater potential for major earthquakes than the adjoining regions that have ruptured more recently.

The 28 February 1979 earthquake occurred on the edge of a network of 50 telemetered short-period seismic stations operated by the U.S. Geological

Survey in southern Alaska (6) as part of its seismic hazard assessment program. The closest station is about 35 km from the epicenter of the main shock, and ten stations are within 100 km at azimuths between 130° and 320° clockwise from north. Readings of P body waves were also obtained from three new Canadian stations in the southern Yukon Territory at distances of 150 to 200 km.

Epicenters determined for the main shock and 102 of the larger aftershocks that occurred within the following 6 days are shown in Fig. 1A. Only solutions with estimated epicentral standard errors less than 10 km, root-mean-square arrival-time residuals less than 1 second, and magnitudes 2.5 or larger are shown. Based on the log number versus magnitude distribution for the aftershocks, the data are probably complete above  $M_L$  4.0. Only 42 of the events in Fig. 1A are smaller than  $M_L$  3.5.

In contrast to the high rate of aftershock activity, Fig. 1B shows the epicenters of the 37 events that occurred from 1 September 1978 to just before the main shock. The earthquakes shown were selected by the same criteria as the after-

shocks. These data are complete, however, above about  $M_L$  2.5 and there are only three events above  $M_L$  3.5. No fore-shock sequence is recognized. The pattern of seismicity is similar to that observed since 1974, when detailed monitoring began, with one exception. The cluster of earthquakes near the southeastern corner of the area outlined by dashes in Fig. 1B occurred during late September in a region without previous high activity. Whether this earthquake swarm is related to the 28 February 1979 event is not known.

The focal mechanism for the main shock, as determined from teleseismic and local P-wave first motions, is shown in Fig. 1A. The steeply dipping plane (strike, N77°E; dip, 79°S) is well constrained, while the gently dipping plane (strike, N105°E; dip, 12°N) is poorly constrained. From regional geology and tectonics and the aftershock distribution (7), the gently dipping plane is inferred to be the fault plane and the steeply dipping plane the auxiliary plane. The inferred slip is predominantly reverse dip slip in a north-northwest direction, in close agreement with the direction expected from plate tectonic models (8, 9).

Aftershocks that occur within 1 day of a large earthquake are often used to indicate the extent of the rupture zone (10). Although 6 days of seismic activity are included in Fig. 1A, the distribution of aftershocks during the first day was not substantially different and gives estimated upper bounds for the rupture dimensions of 65 by 80 km. If the initial rupture area were limited to the northern two-thirds of the indicated aftershock area, which includes the two largest aftershocks and the concentration of events near the U.S.-Canadian border, the rupture dimensions would be approximately 50 by 60 km. In the latter case, the southernmost events would be attributed to secondary faulting triggered by the main shock. Body wave deconvolution suggests that the rupturing was complex, involving at least three rupturing episodes with a combined rupture length of 50 to 70 km.

General constraints on the overall rupture process were determined from fundamental mode Rayleigh waves recorded at the Alaskan stations Palmer (PMR; distance, 425 km; azimuth, 289°) and Shemya (SMY, 2795 km, 272°) and the  $G_2$  surface wave recorded at Uwekahuna, Hawaii (UWE, 4700 km, 199°) (7). The results of these analyses, which were performed by standard computational techniques (11), are included in Table 1. These results are based on limited data and therefore could not be ade-

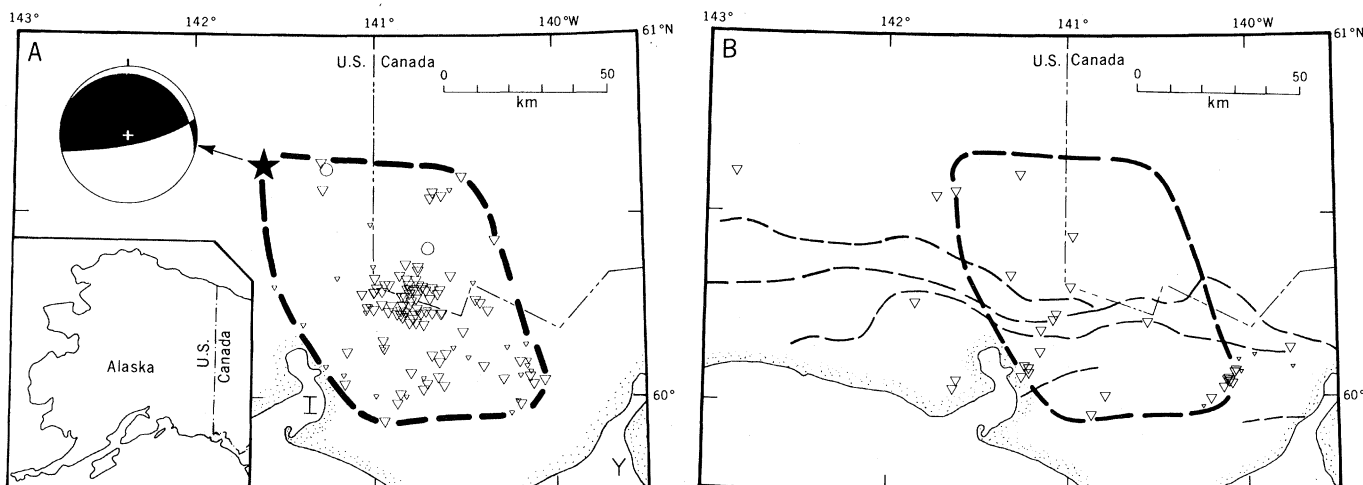


Fig. 1. (A) The 28 February 1979 earthquake (star) and larger aftershocks through 6 March 1979. Circles indicate aftershocks with  $M_s$  greater than 5; triangles indicate aftershocks with  $M_s$  less than 5; small triangles correspond to solutions of poorer quality. Maximum estimate of extent of rupture is indicated by the heavy dashed line. Abbreviations: I, Icy Bay; Y, Yakutat Bay. Lower-hemisphere focal-mechanism solution is shown for main event. Quadrants of compressive P first motion are shaded. (B) Events of  $M_L$  2.5 and greater for the 6 months before main shock. The symbols are as in (A). Light dashed lines correspond to mapped or inferred faults (13).

quately corrected for directivity, multiple wave paths, and variations in source geometry. After more complete analysis, revisions may be possible.

The amplitude spectra of the fundamental mode Rayleigh waves at both PMR and SMY have a conspicuous minimum in the period range of about 30 to 35 seconds. This minimum was modeled by theoretical spectra for a fault oriented as in Table 1, varying the direction and average speed of rupture and the focal depth parameters. Of the three cases considered—unilateral rupture to the west, bilateral rupture to both east and west, and unilateral rupture to the east—only the last gives a minimum in the appropriate period range. Thus, the direction of rupture, as derived by this analy-

sis, agrees with the distribution of aftershock activity. The observed spectra were fitted best by a rupture velocity of 2.5 km/sec and are relatively insensitive to variations in focal depth from about 10 to 30 km. If the rupture length was larger than the 50 km assumed in all the computations referred to above, then this rupture velocity represents a minimum estimate.

The seismic moments ( $M_0$ ) estimated from the fundamental mode Rayleigh waves at PMR and SMY are  $4 \times 10^{27}$  and  $7 \times 10^{27}$  dyne-cm, respectively, in good agreement with the preliminary estimate of  $7 \times 10^{27}$  dyne-cm by Lahr *et al.* (7) based on the  $G_2$  wave recorded on the east-west component at UWE. The seismic moment calculated by deconvolu-

tion of teleseismic body waves was  $1.2 \times 10^{27}$  dyne-cm—approximately three to six times smaller than the surface wave moments. Taking the rupture area ( $A$ ) as  $65 \text{ km} \times 80 \text{ km}$ , or  $5 \times 10^{13} \text{ cm}^2$ , and the rigidity ( $\mu$ ) as  $4 \times 10^{11} \text{ dyne/cm}^2$ , we obtain an estimated average fault displacement ( $M_0/\mu A$ ) of 0.6 to 3.5 m. The smaller rupture area estimate,  $60 \text{ km} \times 50 \text{ km}$ , would imply a displacement of 1.0 to 6 m.

The average rupture depth was estimated by using the P and S body waves recorded at Palisades, New York. An sS minus S delay of 6 seconds and an sP minus P delay of 5 seconds gave the least deconvolutional noise, fixing the average rupture depth at approximately 11 km. This is consistent with a main shock hypocenter at somewhat greater depth and rupture upward toward the surface. Arrival-time data for the main shock and aftershocks constrain the depths to less than about 25 km.

The February earthquake ruptured only the eastern quarter of the identified seismic gap. A larger earthquake may therefore rupture the large remaining seismic gap between Icy Bay and Kayak Island. According to the analysis by Plafker and Ruben (12) of the terraces on Middleton Island, uplift of about 3.5 m, similar to that during the 1964 Alaska earthquake, should occur again within a relatively short time compared to the time required to cut a terrace. This implies that a gap-filling event may also reactivate the easternmost part of the 1964 rupture zone and produce the postulated uplift of Middleton Island. Even if the entire seismic gap was relieved of stress by the 1899–1900 sequence of events,

Table 1. Preliminary estimates of source parameters of the Saint Elias earthquake of 28 February 1979.

Parameter	Size and uncertainty	Comments
Origin time	21:27:06.1 UT	Determined from U.S. and Canadian regional network data
Epicenter	$60^\circ 38.6' \text{N} \pm 2'$ $141^\circ 35.6' \text{W} \pm 1'$	
Depth	$15 \pm 10 \text{ km}$	Lahr <i>et al.</i> (3)
Preferred fault plane		
Dip angle	$12^\circ \text{N} \pm 3^\circ$	
Azimuth of relative slip motion	$\text{N}13^\circ \text{W} \pm 3^\circ$	
Strike	$105^\circ + 5^\circ, -10^\circ$	Least well determined of P-nodal parameters
Fault length	60 to 80 km	
Fault width	50 to 65 km	
Average rupture velocity	2.5 km/sec	To east-southeast of epicenter
Seismic moment	$6 \pm 4 \times 10^{27} \text{ dyne-cm}$ $7 \pm 5 \times 10^{27} \text{ dyne-cm}$ $1 \pm 0.4 \times 10^{27} \text{ dyne-cm}$	Rayleigh waves at PMR and SMY* $G_2$ at UWE Body phases at HKC, ESK, KEV, and PAL

\*Locations of seismic stations: PMR, Palmer, Alaska; SMY, Shemya, Alaska; UWE, Uwekahuna, Hawaii; HKC, Hong Kong; ESK, Eskdalemuir, Scotland; KEV, Kevo, Finland; and PAL, Palisades, New York.

continued convergence at a rate of 5 cm/year could have produced potential slip of 4 m. That amount of slip, if released today in one event, might generate a magnitude 8 earthquake in the remainder of the gap.

No specific premonitory phenomena are recognized at present in this region. McCann *et al.* (3) imply that the gap may be the site of a major earthquake within the next few years, based on the spatial-temporal pattern of earthquakes during the past 20 years. However, the timing could be affected by earthquakes in adjacent regions. For example, a major earthquake on the Denali-Totschunda-Chatham Strait fault system, which lies to the north and east, might partly relieve the stress within the gap, thus increasing the time until the next large earthquake. Nevertheless the region between Kayak Island and Icy Bay appears to be among the most likely sites for the next major earthquake in the United States. As such, the area should be the site of intensified observations, both for earthquake prediction and for studies of strong ground motion.

J. C. LAHR, C. D. STEPHENS  
United States Geological Survey,  
Menlo Park, California 94025

H. S. HASEGAWA  
Earth Physics Branch, Department of  
Energy, Mines and Resources,  
Ottawa, Ontario, Canada K1A 0Y3

JOHN BOATWRIGHT  
Lamont-Doherty Geological  
Observatory of Columbia University,  
Palisades, New York 10964

#### References and Notes

1. U.S. Geol. Surv. Prelim. Determination Epicenters No. 7-79 (1979).
2. W. Thatcher and G. Plafker, *Int. Union Geod. Geophys. IASPEI/IAVCEI Assem. Abstr.* (1977), p. 54.
3. W. R. McCann, O. J. Pérez, L. R. Sykes, *Science* **207**, 1309 (1980).
4. D. G. Tobin and L. R. Sykes, *J. Geophys. Res.* **73**, 3821 (1968).
5. J. A. Kelleher, *ibid.* **75**, 5745 (1970); L. R. Sykes, *ibid.* **76**, 8021 (1971).
6. C. D. Stephens, J. C. Lahr, K. A. Fogleman, M. A. Allan, S. M. Helton, *U.S. Geol. Surv. Open-File Rep.* 79-718 (1979).
7. J. C. Lahr, G. Plafker, C. D. Stephens, K. A. Fogleman, M. E. Blackford, *U.S. Geol. Surv. Open-File Rep.* 79-670 (1979).
8. J. C. Lahr, thesis, Columbia University (1975).
9. J. B. Minster and T. H. Jordan, *J. Geophys. Res.* **83**, 5331 (1978).
10. H. Kanamori, *ibid.* **82**, 2981 (1977).
11. Y. B. Tsai and K. Aki, *ibid.* **75**, 5729 (1970); A. Ben-Menahem, *Bull. Seismol. Soc. Am.* **51**, 401 (1961).
12. G. Plafker and M. Rubin, *U.S. Geol. Surv. Open-File Rep.* 78-943 (1978), p. 687.
13. T. R. Bruns and G. Plafker, *U.S. Geol. Surv. Open-File Map* 75-508 (1975).
14. We thank R. A. Page and J. C. Savage for critically reading this report. This study was partly supported by the Outer Continental Shelf Environmental Assessment Program of the National Oceanic and Atmospheric Administration. This is Canadian Department of Energy, Mines and Resources Contribution 802.

18 June 1979; revised 8 November 1979

## High-Pressure Phase in Americium Metal

**Abstract.** *X-ray diffraction studies at high pressure (above 150 kilobars) show that americium metal undergoes a phase change from a high-symmetry, face-centered cubic structure to an orthorhombic  $\alpha$ -uranium structure. This transition results from the onset of *f*-electron bonding as the lattice is compressed.*

Studies on americium metal (1) have shown two stable structures at atmospheric pressure: a high-temperature, face-centered cubic (fcc) structure and a low-temperature (< 700°C) double hexagonal-close-packed (dhcp) phase. Stephens *et al.* (2) measured compressions to 30 kbar of samples containing both the fcc and dhcp forms. Akella *et al.* (3) reported an fcc structure at 65 kbar with a lattice constant of 4.684 Å. Our work extends compression values for americium metal to much higher pressures (~ 160 kbar) and reveals a third phase, the orthorhombic  $\alpha$ -uranium structure. Since americium is the first actinide element to have nonbonding *f* electrons, this transition demonstrates that these *f* electrons can be forced to participate in the bonding under pressure.

Our sample contained 2000 parts per million (ppm) of ytterbium and less than 100 ppm of other impurities. Normally pure americium has the dhcp structure under ambient conditions. The presence of the ytterbium in our sample allowed the high-temperature fcc phase to be retained after quenching (4).

The experimental apparatus included a diamond anvil cell with a film cassette described by Bassett *et al.* (5). The diamonds had a culet diameter of 600  $\mu$ m. A 265- $\mu$ m-thick gasket (Inconel X-750) preindented to 60  $\mu$ m was used with a hole diameter of 190  $\mu$ m. The sample chamber formed by the hole in the gasket and the diamond tips contained the ytterbium-stabilized americium sample, sev-

eral single-crystal ruby chips and powdered aluminum for the pressure calibration measurements, and silicone diffusion pump oil to serve as a quasi-hydrostatic pressure medium.

Pressures were measured by the ruby fluorescence method (6) before and after each film exposure (except for the measurements at 177 kbar). After pressure changes, the cell was allowed to relax for at least 1 day before any data were taken. For each pressure measurement, a ruby chip from the original supply was used as a temperature standard at 1 bar to eliminate errors due to possible temperature shifts in the fluorescence lines. The compression of the powdered aluminum seen in the high-pressure diffraction patterns provided a check on the sample-to-film distance. Independent pressure determinations from the ruby fluorescence and aluminum diffraction lines were in good agreement within their respective error limits.

All x-ray diffraction patterns were made with Mo K $\alpha$  radiation (wavelength  $\lambda = 0.7107$  Å) and were recorded on Kodak Industrex AA film. The x-ray tube was operated at 45 kV and 20 mA, and exposure times were 500 to 600 hours. After the films were developed, they were scanned and their density values digitized. In this form the data were then processed with an image enhancement computer program (7); an additional enlargement was made to simplify measurements of the  $2\theta$  diffraction angles.

Diffraction films were obtained at

Table 1. Structural data for americium metal at pressure.

Pressure (kbar)	Structure type	Lattice constants (Å)	Unit cell volume	Atomic volume
0	fcc	$a = 4.894$	117.15	29.29
65*	fcc	$a = 4.684$	102.77	25.69
152 $\pm$ 2	Orthorhombic $\alpha$ -uranium	$a = 3.063 \pm 0.004$ $b = 5.968 \pm 0.010$ $c = 5.169 \pm 0.008$ $y = 0.1025 \pm 0.0025$	94.49	23.62
161 $\pm$ 2	Orthorhombic $\alpha$ -uranium	$a = 3.060 \pm 0.005$ $b = 5.962 \pm 0.011$ $c = 5.155 \pm 0.008$ $y = 0.1025 \pm 0.0025$	94.04	23.51
177 $\pm$ 2	Orthorhombic $\alpha$ -uranium	$a = 3.046 \pm 0.004$ $b = 5.957 \pm 0.009$ $c = 5.148 \pm 0.007$ $y = 0.1025 \pm 0.0025$	93.41	23.35

\*From Akella *et al.* (3).